NATIONAL ADVISORY COMMITTEE FOR AERONAUTICS

TECHNICAL MEMORANDUM NO. 606

FLAT SHEET METAL GIRDERS WITH VERY THIN METAL WEB*

By Herbert Wagner

PART III

Sheel Metal Girders with Spars Resistant to Bending — The Stress in Uprights — Diagonal Tension Fields

The actually occurring form change is of course not identical with our arbitrarily assumed one. The principal difference may be the change in specific number of wrinkles from direction x to z, so that b and, according to equation (29b) (See Part I – Technical Memorandum No. 605, page 32), f, become variable in direction z. Moreover, it seems likely that b and f increase from the edge toward the center if the sheet is infinitely thin.

The work of deformation A, actually produced is, however, certainly less (equal in the limiting case) than in that arbitrarily assumed, and must therefore (Compare eq. 31, Technical Memorandum No. 605, page 35), equal A_{min}. But from this it follows (eq. 31a) that this actual deformation is under constant tension stress $\sigma = \frac{\Delta z}{h} E = \epsilon E$ and that there are no additional stresses of finite magnitude in this zone; that is, $-\sigma_{qk}$ and

$\sigma_b = 0$. Now $-\sigma_{qk} = 0$ and $\epsilon = \dfrac{\sigma}{E}$ were precisely the two fundamental assumptions for calculating the diagonal tension fields. The calculation of the work of deformation for the arbitrarily chosen deformation presents no difficulties, and we can pass to the boundary $E\dfrac{s^2}{h^2} \longrightarrow 0$. Selecting the dimensions which characterize the attitude of the form change in the limiting case according to inequation (32a) - (Technical Memorandum No. 605, page 38) then yields $A = A_{min}$.

We briefly indicate this calculation for the case of oblique wrinkles, and for that purpose resort to Figure 33, which shows a sheet metal girder with x and y as the coordinates of the plane of the sheet. Upper and lower spars are to be parallel to axis x. The lateral edge members are considered very far apart and not within the range of our consideration. Now we subject the spars to elongation ϵ_{xo} in the direction of x and raise their distance in direction y by $h\,\epsilon_{yo}$. In addition, we shift the upper spar by $h\,\gamma_0$ to the right with respect to the lower spar. This causes the sheet to wrinkle, its components undergo displacements ξ in direction x and displacements η in direction y and bulge by ζ out of the original plane of the sheet.

Now the deformations of the arbitrarily chosen form change are defined as:

$$\xi = \epsilon_{xo}\, x + \gamma_0\, y + \frac{1}{8}\, e\, \varphi^2\, [\sin\, 2\, e\, (x - y \cot \alpha)]$$

$$\eta = \epsilon_{yo}\, y - \frac{1}{8}\, e\, \varphi^2\, \cot \alpha \, \sin\, [2\, e\, (x - y \cot \alpha)]$$

$$\zeta = \varphi\, \cos\, [e\, (x - y \cot \alpha)].$$

where α = angle of direction of wrinkles,

$e = \dfrac{\pi \sin \alpha}{b}$ (b = half width of wrinkle)

φ = depth of wrinkle in culmination point.

We select φ in conformity with the discussion for Figure 32. With f as the depth of the wrinkles in the mean range of the sheet, we write for the sheet restrained at the edge:

$\varphi = \dfrac{1}{2} f[1 - \cos \dfrac{\pi z}{r}]$ within range of $z = 0$ to $z = r$,

$\varphi = f$ within range of $z = r$ to $z = h - r$,

$\varphi = \dfrac{1}{2} f[1 - \cos \dfrac{\pi(h - z)}{r}]$ within range of $z = h - r$
    to $z = h$.

Then we compute the work of the form change for a component of base $d_x d_y$ (for example, according to Föppl, Drang und Zwang, Vol. 1, 1920, pp. 130 and 154). This work consists of bending stresses and the mean stresses in tension and shear, so the total work is integrated over the entire area of the sheet. It is advisable to integrate first in direction x and then in direction y conformal to the three ranges.

Aside from the given dimensions of the sheet and the three quantities ϵ_{xo}, ϵ_{yo} and γ_o defining the deformation of the edges, the equation contains only the four quantities α, b, f and r, which characterize the wrinkling. So a partial differentiation of the work of form change yields only four equations. For $E \dfrac{s^2}{h^2} \rightarrow 0$ these equations are complied with when

1) every ratio of $\dfrac{r}{b}$, which satisfies (32), is likewise conformable for every finite $\dfrac{r}{b}$ for instance,

2) $\tan 2\,\alpha = \dfrac{\gamma_0}{\epsilon_{xo} - \epsilon_{yo}}$

3) $2\,m\,\dfrac{\pi^2 f^2}{4 b^2} = (m - 1)\,\dfrac{\gamma}{\sin 2\,\alpha} - (m + 1)(\epsilon_{xo} + \epsilon_{yo})$,

4) $\dfrac{b}{h} = 0.$

This is in perfect agreement with (4) and (39b).*

The number of wrinkles or their exact form are not calculated, since that is of no particular interest to us. But it is essential that the wrinkles in infinitely thin sheets are such that our fundamental assumptions (particularly $-\sigma_{qk} = 0$) for the whole range of the sheet, with the exception of the edges, be correct, and that σ_b vanishes in the infinitely thin sheet.

Now the assumptions which we made previously, constitute, in fact, the exact theory for calculating the stresses in infinitely thin wrinkled sheets when it is a question of defining these stresses within the field. The deviations at the edges are of finite magnitude, although we are unable to give accurate data on their behavior. But, owing to the infinitely small range within which these deviations occur, and their correspondingly infinitely little work of form change, their effect on the amount of form change in the girder is zero, regardless of whether the sheet is restrained at the edge or simply freely supported.

According to experiments new wrinkles interspace themselves on the edges, so that there are more wrinkles on the

edges than in the middle. In this way the depth of the wrinkles decreases toward the edge, without effecting a like increase in cross stress $-\sigma_{qk}$. It is only at the edge itself that the stresses parallel to the spar (aside from $\frac{\sigma \sin^2 \alpha}{m}$) equal the stress in the spar.

Determination of Experimental Error

Now we figure back from the deformations determined by test, in order to see the extent of applicability of our assumption $\sigma_q = 0$ to practical cases; then we compute σ_b.

From (Fig. 7 of my report given at Danzig, Jahrbuch 1928, der Wissenschaftlichen Gesellschaft für Luftfahrt, p. 115,) the width b of a wrinkle with respect to its length l and girder height h can be measured quite accurately. In the left panel we have

$l = 18$ (= length of wrinkle from upright to upright),

$\left.\begin{array}{l} b = 2.8 \\ s = 0.025 \end{array}\right\}$ $s/b = 0.0089.$

In addition:

$E = 700,000$ kg/cm²

$\sigma = \quad 2,400$ "   consequently $\epsilon = 0.0034$

$\sigma_y = -1,600$ "   " $\epsilon_y = -0.0023$

$\sigma_x = -\quad 300$ "   " $\epsilon_x = -0.0004$

Equation (28) yields:

$$\sigma_{qk} = - \frac{\pi}{12} E \left(\frac{s}{b}\right)^2 = - 46 \text{ kg/cm}^2.$$

which is only 2 per cent of σ.

Moreover, the depth of the wrinkles is not perfectly constant, not even in the center. The tension stress σ of the plate fiber running in the culmination line (Section 1, Fig. 34) calls, on account of the curvature of this fiber (due to equilibrium of components acting perpendicular to the sheet), for a compression stress σ_{qD} perpendicular to σ (hence in direction of σ_{qk}) which is computed at:

$$\sigma_{qD} = - \sigma \frac{\sigma_q}{\sigma_z}.$$

σ_z and σ_q are the radii of curvature of the wrinkles (Fig. 34). Assuming the wrinkle in section 1 of Figure 34 to be pure sinusoidal, $(\zeta = f \sin \frac{\pi z}{l})$, the value for σ_{qD} is surely too high:

$$\sigma_{qD} = - \sigma \frac{b^2}{l^2} ,$$

and with our figures

$$\sigma_{qD} = - 2400 \times 0.024 = - 58 \text{ kg/cm}^2.$$

So σ_{qD} is certainly lower than 2.4% of σ. For total cross stress we have at the highest

$$\sigma_q = \sigma_{qk} + \sigma_{qD} = - 104 \text{ kg/cm}^2,$$

that is, 4.4% of σ.

Conforming to the equilibrium of the inside with the outside stresses at a cut through the sheet wall parallel to the uprights we must have:

$$\sigma_q + \sigma_z = \sim \frac{2Q}{hs}.$$

For this case equation (9) yields values which are about 4 per cent too high for σ. If we take the highest stress τ as decisive for the stress of the material, it nevertheless indicates the material stress correctly, because

$$\tau = \pm \frac{1}{2}(\sigma - \sigma_q).$$

Now we define the stress in bending. Equation (5c)[*] yields for

$$\epsilon_q = - \epsilon + \epsilon_x + \epsilon_y = - 0.0061,$$

and (29a):

$$\frac{f}{b} = \frac{2}{\pi} \sqrt{0.0061 - \frac{1}{3.3} \times 0.0034 - 0.0000} = 0.045$$

$$f = 0.126 \text{ cm.}$$

So with (30) we obtain:

$$\sigma_b = \pm \frac{\pi^2}{2} E \, 0.0089 \times 0.0045 = \pm 1400 \text{ kg/cm}^2.$$

The stress in bending is now more than half as high as σ, causing the material to reach its yield limit sooner than our calculation with σ calls for.

The elongation in direction z is the same at I and II (Fig. 34) so that the stress σ in direction z changes by

[*]See equation (5c), Part I, T. M. No. 604, page 32.

$\frac{1}{m} \sigma_b$ at these points, that is, σ decreases at I and increases at II. With $m = 3.3$

$$\sigma_I = 2400 - \frac{1}{m} 1400 = 1980 \text{ kg/cm}^2,$$
$$\sigma_{II} = 2400 + \frac{1}{m} 1400 = 2820 \text{ kg/cm}^2.$$

To illustrate the effect of σ on the stress in the material we discuss two limiting cases:

1) The greatest elongation is to be decisive for the stress in the material. Since, as we just stated, the bending stress σ_b has no effect on the elongation in direction z, the reduced stress $\sigma_r = \sigma = 2400 \text{ kg/cm}^2$. There is no change in material stress.

2) The highest shear stress is to be decisive for the stress in the material. The maximum occurs at point I and amounts to $\tau_{max} = \frac{1}{2}(\sigma_I + \sigma_b) = \frac{1}{2}(1980 + 1400) = \frac{1}{2} \times 3380 \text{ kg/cm}^2$, as against $\tau_{max} = \frac{1}{2} \times 2400$, if $\sigma_b = 0$. According to this the yield limit is reached at I, while the tension σ amounts to only 70 per cent of the yield limit.

The difficulty in bringing out the premature reach of yield limit by tests is obviously due to the small range within which the stresses become appreciably higher than the simple theory defines. Then it may be due in part to a higher yield limit in the outer layer of the sheet, or to the uprights which together with the spars have a boxlike effect to a certain degree, and

thus reduce the cross section in the plate. It is also possible that our assumption of τ_{max} as decisive for the material stress was, after all, perhaps a little too unfavorable for our case.

We again repeat that the theory developed for the diagonal tension field simply postulates that $\sigma_q = 0$ and that $\epsilon = \frac{\sigma}{E}$; we do not presume σ_b to be very low. Hence, stress σ calculated on these premises yield the exact mean tension stress (the mean formed over plate thickness σ) regardless of the relatively high σ_b.

Moreover, it should be noted that $\frac{\sigma_b}{\sigma}$ is presumed to be low only when the plates are actually thin compared to their other dimensions. Even if the stress, at which wrinkling sets in, is not materially below the yield limit (not lower than 1/50 of the yield limit, for instance), the plate soon reaches this critical point, after wrinkling.

As $s \rightarrow 0$, σ_b diminishes very slowly like $\alpha^{\kappa-\beta}$ and can actually be counted upon as being very low for very thin plates.

Lastly, we examine the differences in tension stress σ, which result when the sheet fiber running in the direction of the culmination line of the wrinkle is stretched more than the fiber which (almost) remains in its original plane. Again, assuming the culmination line as sinusoidal, the comparative elongation in this line is

$$2 \, \Delta \, \epsilon = \frac{\pi^2}{4} \, \frac{f^2}{l^2}$$

greater than in the fiber remaining in its initial plane.   Hence
we may presume that the first stretches $\Delta \epsilon$ more and the other
$\Delta \epsilon$ less than $\epsilon = \dfrac{\sigma}{E}$,   so that:

$$\Delta \sigma = E \Delta \epsilon = 42 \text{ kg/cm}^2,$$

which is not quite 2 per cent of σ.

In the center of the field the actually prevailing fluc-
tuation in stress is presumably less than the calculated figure,
but certainly higher at the edge, although no marked deviations
from σ are to be anticipated even at the edge.

Exceeding the Yield Limit

Here we merely consider the case of the web plate when
exceeding the yield limit. We have already stated that, prior
to reaching this limit, the material begins to break down at
different places, due to the local bending stresses σ_b. But
owing to the limited range (if the bending stresses become at
all noticeable) they have no effect on the deformations of the
whole girder nor on the mean tension stress σ.

Only when σ itself reaches the yield limit, does the
stress show a slight change. Equations (4), (5) and (18) re-
main, in so far as they represent relations between α, β, γ,
ϵ, ϵ_q, ϵ_x, ϵ_y, and ϵ_v, applicable. After exceeding the yield
limit in the web plate ϵ preponderates over ϵ_x and ϵ_y,
and we approximate $\alpha = 45^\circ$ ($\alpha = \beta/2$) and $\gamma = 2\epsilon$. Now

when we write these values in (9) and (18) we have for perpendicular uprights

$$\sigma = \frac{2Q}{hs}$$

and

$$\sigma = \frac{2Q}{hs} \cot \beta/2$$

for oblique uprights. For the first type this agrees with (13a), but with $\alpha = 45^\circ$ we have:

$$-V = Q\frac{t}{h} .$$

So if the dimensions of the web plate are such that the yield limit is exceeded by ultimate load, equation (13b) is inapplicable for computing the uprights, or the V values would become too low.

σ_{qk} decreases after the yield limit has been exceeded, so that the assumption $\sigma_{qk} = 0$ applies now even better than before exceeding the limit. The bending stresses σ_b as well as the fluctuations in stress $\Delta \sigma$ disappear, and so have no effect on the ultimate load. If σ_B is the tearing strength of the sheet, the ultimate load Q_B of the web plate is always computed at

$$Q_B = \frac{1}{2}\sigma_B \, hs \tan \beta/2,$$

provided, the box effect of the uprights is small.

General Diagonal Tension Fields —

Transverse Contraction

The rectangular, very thin unstressed sheet (Fig. 35) is deformed as follows: we subject the sheet in the direction of axis n to a constant transverse contraction $-\epsilon_{qo}$, or in other words, produce wrinkles in the direction of axis z.

Now we apply tension stresses at the edges B, these stresses to increase linearly with n in direction n:

$$\sigma = \sigma_0 + \frac{d\sigma}{dn}\, n.$$

The result is an (infinitely small) curvature of the separate fibers of the sheet (compare equation 2a, N.A.C.A. Technical Memorandum No. 604, Part I). But since we assumed $\frac{d\sigma}{dn} =$ constant, the curvature of all these fibers is the same; so the distance of two such adjacent fibers remains constant, hence transverse contraction $-\epsilon_q = -\epsilon_{qo}$ remains constant. Then we subject the sheet (Fig. 36) to an identical transverse contraction $-\epsilon_{qo}$, and again apply tension stresses σ at the edge in direction z. But now they are to increase irregularly as indicated on Figure 36. The curvature radii $-\sigma = \frac{1}{E}\frac{d\sigma}{dn}$ (compare equation 2a) of the individual fibers running in direction z are now different (see Fig. 36). The fibers, originally exactly in direction z, are now exactly perpendicular after the deformation.

If we took care when applying tension stress σ that the transverse contraction remained unchanged at the edges, (that is $-\epsilon_{qo}$) the contraction $-\epsilon_q$ in the middle range of the sheet must now differ from the original $-\epsilon_{qo}$. This means lower at C because here the fibers are farther apart than at the edge; at D the contraction is now greater than $-\epsilon_{qo}$.

Thus it will be seen that the transverse contraction is capable of changing along a wrinkle and may assume extreme (maximum or minimum) values even in the middle range of a wrinkle. So when we define the validity of inequation (2), (see Part I, N.A.C.A. Technical Memorandum No. 604,) it must include the whole range of the sheet, not merely the edges.

But it may occur in a sheet with relatively low $-\epsilon_{qo}$ (Fig. 36), that inequation (2) is satisfied at the edges but not in the dotted range around C, in which case our assumptions would have to be disregarded for other more complicated ones. But in our further discussion we consider (2) to be complied with in the whole range.

Figure 36 shows σ constant and $-\epsilon_q$ variable along the wrinkles, consequently the depth with respect to the width of the wrinkle must vary along its length according to (29b) (see Part II, N.A.C.A. Technical Memorandum No. 605); the wrinkled sheet presents no developable surface and it may be inferred that the sheet would resist this type of wrinkling. But it be proved that in an infinitely thin sheet with very (infinitely)

low depth of wrinkles this resistance to wrinkling disappears
even in this case, so that our presupposed deformation attitude
yields the least work of deformation.

Now we subject the sheet in Figure 37 to a transverse
contraction $-\epsilon_{qo}$, after which we again apply tension stresses
σ, which on the left we allow to increase linearly up to the
center, and on the right to decrease linearly. In the center
itself $\frac{d\sigma}{dn}$ is unsteady, that is, $\frac{d^2\sigma}{dn^2}$ is infinitely great.
When we plot the fibers running in direction z after the
deformation, we find that the two fibers infinitely close to
the right and left of the center would have to intersect after
deformation. But this is not actually possible because the
connection of the sheet must be kept intact; these two fibers
must, in fact, run parallel to the center line. The fibers
originally in direction Z near point M can therefore be no
longer exactly perpendicular to the sheet edges after the def-
ormation. This means there must be shear stresses acting in the
direction of and perpendicular to the wrinkles, which effect this
change in angle. Our basic assumption of zero shear stress in the
direction of the wrinkles no longer holds true in the range
around point M, and we must presuppose that the edges are sub-
jected to steady deformation.

General Stress and Deformation Attitude of a Tension Diagonal

We resume our earlier discussion on the attitude of stress in a diagonal tension field. Figure 38 shows a plate strip between two stress trajectories which we call, for short "tension diagonal." Axis z is placed in the direction of the strip. At $z = 0$, that is, point M, the width of the strip is given - $\overline{MM_1} = dn_m$. The angle formed by the stress trajectory passing through M with the x-axis passing through M, we call α. The stress trajectory passing through M_1 forms with axis x the angle $\alpha + \frac{\partial \alpha}{\partial n_m} dn_m$, which usually differs from α; the angle of the two stress trajectories enclosing the strip is $\frac{\partial \alpha}{\partial n_m} dn_m$.

Other given data are, the principal tension stresses σ_m in point M and

$$\sigma_{m_1} = \sigma_m + \frac{\partial \sigma}{\partial n_m} dn_m \tag{34}$$

in point M_1.

First we define the width dn of the tension diagonal at z (point P). We obtain

$$dn = dn_m \left(1 - z \frac{\partial \alpha}{\partial n_m}\right) \tag{35}$$

Since the term $z \frac{\partial \alpha}{\partial n_m}$ recurs many times in the subsequent calculation, we abbreviated it to r, so that

$$r = z \frac{\partial \alpha}{\partial n_m} \tag{36}$$

where, of course, we must always bear in mind in the subsequent

differentiations and integrations, that r is a function of z. Consequently, equation (35) becomes now

$$dn = dn_m (1 - r) \qquad (35a)$$

Then we calculate the stress attitude of the tension diagonal. In conformity with the freedom from sources in the field of the principal stresses (See Part I - Technical Memorandum No. 604, theorem 2, page 11)

$$\sigma_m \, dn_m = \sigma \, dn \qquad (37)$$

is valid, that is, with (35a):

$$\sigma = \sigma_m \frac{1}{1 - r} . \qquad (37a)$$

Now we compute $\dfrac{\partial \sigma}{\partial z}$, so that (36) yields:

$$\frac{\partial \sigma}{\partial z} = \sigma_m \frac{\frac{\partial r}{\partial z}}{(1 - r)^2} = \sigma_m \frac{\partial \alpha}{\partial n_m} \frac{1}{(1 - r)^2}$$

In particular, we obtain with $z = 0$ and $r = 0$ for point M

$$\left(\frac{\partial \sigma}{\partial z}\right)_{z=0} = \sigma_m \frac{\partial \alpha}{\partial n_m} \qquad (37b)$$

Then the stress becomes

$$\sigma_1 = \sigma + \frac{\partial \sigma}{\partial n} \, dn$$

in point P_1. Taking into account the infinitely small terms of the first order, we obtain

$$\sigma_1 \, dn = \sigma_{m1} \, dn_m$$

Then we make $\sigma_1 - \sigma = \dfrac{\partial \sigma}{\partial n} \, dn$ (Fig. 38), that is, with the pre-

ceding equation

$$\frac{\partial \sigma}{\partial n} dn = \sigma_1 - \sigma = \sigma_{m1} \frac{dn_m}{dn} - \sigma$$

and obtain with equations (34), (37) and (35a):

$$\frac{\partial \sigma}{\partial n} = \frac{\partial \sigma}{\partial n_m} \frac{1}{(1 - r)^2} \qquad (38)$$

Now σ and its derivations conformal to z and n are known at every point of the tension diagonal.

With

$$\epsilon = \frac{\sigma}{E} , \qquad (39)$$

that is, particularly when, for example,

$$\epsilon_m = \frac{\sigma_m}{E} , \text{ etc.,} \qquad (39a)$$

it becomes apparent that all these equations are applicable to the elongations, providing we write ϵ instead of σ.

Now we calculate the form into which the originally straight fiber which passes through M and coincides with the stress trajectory changes when subjected to the discussed tension stresses. We emphasize that this form depends only on those tension stresses, but not on the transverse contraction.

Beginning with the increase λ_z in the distance of two points O and U (Fig. 39) caused by tension stress σ and elongation ϵ, equation (37a) yields:

$$\lambda_z = \int_{z_1}^{z_2} \epsilon \, dz = \int_{z_1}^{z_2} \frac{\epsilon_m}{1 - r} \, dz,$$

and equation (36) yields

$$\lambda_z = \frac{\epsilon_m}{\frac{\partial \alpha}{\partial n_m}} \ln \frac{1 - r_2}{1 - r_1} \tag{40}$$

when $r_1 = z_1 \frac{\partial \alpha}{\partial n_m}$, etc.

In case $z_2 = - z_1$ (Fig. 39a), we have

$$\lambda = \frac{\epsilon_m}{\frac{\partial \alpha}{\partial n_m}} \ln \frac{1 + r_1}{1 - r_1} \tag{40a}$$

Conformably to equation (2a) (Part I - Technical Memorandum No. 604) the fiber curves. If v is the displacement of a point in direction n, caused by the deformation of the fiber, equation (2a) yields

$$\frac{\partial^2 v}{\partial z^2} = - \frac{\partial \epsilon}{\partial n}$$

that is,

$$- \frac{\partial v}{\partial z} = \int \frac{\partial \epsilon}{\partial n} \, dz$$

Assuming the fiber to be fixed in M so as to preclude all distortion in this point (38) and (36) yield

$$- \frac{\partial v}{\partial z} = \frac{\frac{\partial \epsilon}{\partial n_m}}{\frac{\partial \alpha}{\partial n_m}} \frac{r}{1 - r} \tag{41}$$

$- \frac{\partial v}{\partial z}$ is the angle formed by the tangent to the fiber in a point F and the tangent to the fiber in point M.

A second integration of (36) yields

$$- v = - \int_0^z \frac{\partial v}{\partial z} \, dz = D \left[\ln \left(\frac{1}{1-r} \right) - r \right] \tag{42}$$

which is briefly written as

$$D = \frac{\frac{\partial \epsilon}{\partial n_m}}{\left(\frac{\partial \alpha}{\partial n_m} \right)^2} \tag{42a}$$

Now we know the form of the fiber in the sheet. But for later purposes we present the data in somewhat different manner. We assume the two points O and U of our tension diagonal isolated and connected by a straight line; then let μ represent the distance of a point on the plate fiber from this line. But we give the result of this simple calculation in a form adapted to our special case of sheet metal girder, namely, for $z_2 = - z_1$ (Fig. 39a). With equation (42a), we have:

$$\mu = D \left[\frac{1}{2} \ln \left(\frac{1}{1 - r_1^2} \right) + \frac{r}{2 \, r_1} \ln \left(\frac{1 + r_1}{1 - r_1} \right) - \ln \left(\frac{1}{1 - r} \right) \right] \tag{43}$$

Then we calculate angle $\frac{\partial \mu}{\partial z}$, particularly at point O and U. We obtain

$$- \left(\frac{\partial \mu}{\partial z} \right)_{0,U} = \frac{\frac{\partial \epsilon}{\partial n_m}}{\frac{\partial \alpha}{\partial n_m}} \left[\frac{1}{1 \mp r_1} - \frac{1}{2 \, r_1} \ln \left(\frac{1 + r_1}{1 - r_1} \right) \right] \tag{44}$$

where the upper sign is valid for point O and the lower sign for point U.

This defines the stress attitude of the tension diagonal

and the ensuing form of the diagonal, still leaving the elongation attitude. The elongations ϵ in the z direction are already known from the stress σ, and our problem is to find the elongations perpendicular to it, namely, the transverse contraction $- \epsilon_q$. We could again assume the transverse contraction $- \epsilon_{qm}$ at point M and its derivation according to z as given and compute with these data and the given stress attitude the contraction at the other points of the tension diagonal. But we prefer to use another method, which supplies the result which conforms better to the ordinarily known limit equations. We assume the transverse contractions $- \epsilon_{qo}$ and $- \epsilon_{qu}$ in point O and U given and then define the contraction $- \epsilon_q$ at a point z by applying stresses.

Figure 40 shows the two adjacent plate fibers in unloaded attitude as dotted lines. Their distance at O is $d \, n_o$, and at U, $d \, n_u$. Now we increase this distance by $d \, n_o \, \epsilon_{qo}$ and and $d \, n_u \, \epsilon_{qu}$. The result at z is a raise in distance $d \, n$ amounting to $d \, n \, \overline{\epsilon_q}$. For our special case $z_2 = - z_1$ (36) (that is, $r_1 = z_1 \frac{\partial \alpha}{\partial n_m}$ etc.) yields

$$\frac{(dn \, \epsilon_q)}{d \, n} = \overline{\epsilon_q} = \frac{\epsilon_{qo} + \epsilon_{qu}}{2} + \frac{\epsilon_{qo} - \epsilon_{qu}}{2} \frac{r - r_1^2}{(1 - r) \, r_1} \qquad (45a)$$

Moreover, the distance of both adjacent fibers becomes greater, because these fibers can bend differently, that is, by $\mu_1 - \mu$ (Fig. 40). It is

$$\mu_1 - \mu = \frac{\partial \mu}{\partial n} \, dn = (\epsilon_q - \overline{\epsilon_q}) \, dn$$

Now equations (45a) and (35a) yield the whole transverse contraction, as

$$- \epsilon_q = - \frac{\epsilon_{qo} + \epsilon_{qu}}{2} - \frac{\epsilon_{qo} - \epsilon_{qu}}{2} \frac{r - r_1^2}{r_1 (1 - r)} - \frac{1}{1 - r} \frac{\partial \mu}{\partial n_m} \quad (45b)$$

where for $\frac{\partial \mu}{\partial n_m}$ from (43), equation (42a) yields:

$$\frac{\partial \mu}{\partial n_m} = \frac{\mu}{D} \frac{\partial D}{\partial n_m} + \frac{D}{\frac{\partial \alpha}{\partial n_m}} \frac{\partial^2 \alpha}{\partial n_m^2} \frac{r_1^2 - r^2}{(1 - r_1^2)(1 - r)} \quad (45c)$$

To prove the real significance of our considerations on the stress in the tension diagonal, we must check the validity of inequation (2), Part I (Technical Memorandum No. 604, page 7) at O and U, and whether $- \epsilon_q - \frac{\epsilon}{m}$ assumes, perhaps, a minimum along this tension diagonal, as well as whether equation (2) (Technical Memorandum No. 604) is equally complied with at this point.

We know the elongations in direction z and n, and angle $\frac{\partial v}{\partial z}$ formed in a point P by the two fibers running originally in these two directions with the fibers of point H running in those directions. Then we calculate the elongation ϵ_α at point P according to a fiber running at arbitrary angle α_z to the z direction (Fig. 41), and the distortion γ_α of this fiber through this deformation attitude relative to the direction of the tension diagonal in point P. These questions were discussed in Part I (Compare equation (3a):

$$\epsilon_\alpha = \epsilon \cos^2 \alpha_z + \epsilon_q \sin^2 \alpha_z,$$
$$\gamma_\alpha = \sin \alpha_z \cos \alpha_z (\epsilon - \epsilon_q).$$

Moreover, if for point O and U, aside from ϵ_O and ϵ_u we know elongation ϵ_{α_O} and ϵ_{α_u} in a second direction, which forms angle α_O and α_u with direction z, the above equations yield upon elimination of ϵ_q

$$\gamma \, \alpha_O = \cot \alpha_O \, (\epsilon_O - \epsilon_{\alpha_O}), \quad \text{for point} \quad O \qquad (46a)$$

$$\gamma \, \alpha_U = \cot \alpha_U \, (\epsilon_U - \epsilon_{\alpha_U}), \quad \text{"} \quad \text{"} \quad U \qquad (46b)$$

Now we shall add one more consideration which at the same time serves as a sort of introduction to the next paragraph. Figure 42 shows the discussed sheet fiber in its original position as well as a line g_O going through point O, which together with the direction of the fiber forms an angle α_O. When we subject the sheet to stresses, the two points O and U assume a new position, say O_I and U_I, so that the line connecting these two points is distorted by an angle ϑ. Being stressed, the line g_O also shifts to a new position g_{O_I} and the problem is to ascertain the amount of angle ω_O formed by g_O and g_{O_I}. With our previous designations (Fig. 39), it becomes apparent from Figure 42 that

$$(180 - \alpha_O) + \omega_O = \vartheta - \left(\frac{\partial \mu}{\partial z}\right)_O + (180 - \alpha_O) + \gamma \, \alpha_O,$$

so that

$$\omega_O = \vartheta - \left(\frac{\partial \mu}{\partial z}\right)_O + \gamma \, \alpha_O \qquad (46c)$$

and as distortion of a line g_U through point U

$$\omega_U = \vartheta - \left(\frac{\partial \mu}{\partial z}\right)_U + \gamma \, \alpha_U \qquad (46d)$$

$\gamma\alpha_O$ and $\gamma\alpha_U$ conform to equations (46a) and (46b).

Boundary Equations

Example: Sheet metal girder with parallel spars not rigid in bending

The girder in Figure 43 is assumedly constrained at one side and subjected to a stress Q, with the ensuing deformations as shown in Figure 43. The upper spar is under compression, and the lower spar subject to tension stresses; the whole girder deflects. The deformations caused by the cross stresses change the stressed skin into a diagonal tension field; as a result of the tension stresses on the spars, the latter buckle between the uprights; the uprights are compressed. All these deformations are considered as infinitely small in the sense of the conventional assumptions of the strength theory.

But owing to the irregular deformations of the spars, the wrinkles (tension stresses) are now no longer parallel, but vary by a finite amount for the individual wrinkles; α as well as σ and $-\epsilon_q$ now are variable quantities. To this complicated deformation attitude we then apply the data of the preceding section, page 15.

A sheet metal girder with spars not rigid in bending is subjected to precisely the same angle of displacement γ as one with bending resistant spars because of the effect of cross stress Q. Assuming this angle γ as given, we presume it to be constant within the range of our discussion. Moreover, we con-

sider the compression stress in the uprights as being known and
equivalent. The uprights are to be flexibly attached to the
spars and be without lateral bending stiffness. Lastly, the di-
mensions of upper and lower spars are to be such that the elon-
gations ϵ_{xo} and ϵ_{xu}, caused by the spar stresses, are constant.
Our problem then shall be to define the discrepancies between
these two different types of spars.

In Figure 43 the center axis of the girder is denoted by
x_m. Axes x_o and x_u are parallel to x_m and $h/2$ distant
than where the spars are to be. Stresses and deformations are
indicated by subscripts o, u, and m.

Now, first, we assume the intensity and the direction of
the principal tension stress σ and its ensuing elongation ϵ
as known; that is, σ_m and ϵ_m. This gives us the derivations of
these quantities according to X_m (namely, $\dfrac{d\sigma}{d x_m}$, $\dfrac{d\epsilon}{d x_m}$, $\dfrac{d\alpha}{d x_m}$).

Now it follows from Figure 44 that $d n_m = d x_m \sin \alpha$.
With $\dfrac{\partial \alpha}{\partial z} = 0$, we have

$$\frac{\partial \alpha}{\partial n_m} = \frac{1}{\sin \alpha} \frac{d \alpha}{d x_m} \tag{47}$$

The elongation in direction z at point M_2 is

$$\epsilon_m + \frac{d \epsilon}{d x_m} d x_m = \epsilon_m +$$

$$+ \frac{\partial \epsilon}{\partial n_m} d x_m \sin \alpha + \left(\frac{\partial \epsilon}{\partial z}\right)_{z=0} d x_m \cos \alpha$$

with equations (37b) and (47).

$$\frac{\partial \epsilon}{\partial n_m} = \frac{1}{\sin \alpha} \frac{d\epsilon}{d x_m} - \frac{\cos \alpha}{\sin^2 \alpha} \frac{d\alpha}{d x_m} \epsilon_m \qquad (48)$$

Now we know $\frac{\partial \epsilon}{\partial n_m}$ and $\frac{\partial \alpha}{\partial n_m}$ with respect to ϵ_m and α thereby the whole stress and deformation attitude of the diagonal tension field (aside from the transverse contraction $-\epsilon_q$). In particular, we are given the stress and the deformation in O and U; but it must be emphasized that the values of ϵ_O, ϵ_u, etc., calculated for ϵ_m and α at x_m are at

$$\left. \begin{array}{l} x_O = x_m + \frac{h}{2} \cot \alpha \\[2ex] x_U = x_m - \frac{h}{2} \cot \alpha \end{array} \right\} \qquad (49)$$

We designate by X_m, X_O, and X_u the displacements of the points – originally on axes x_m, x_o, and x_u – perpendicular to the direction of these axes. By virtue of the different elongations ϵ_{xo} and ϵ_{xu} the girder is bent (Fig. 43) at a contingent angle

$$-\frac{\epsilon_{x_O} - \epsilon_{x_U}}{h} = \frac{d^2 X_m}{dx_m^2} = \frac{d^2 X_O}{dx_O^2} = \frac{d^2 X_U}{dx_U^2} .$$

With η_O and η_u as the deflections of the spars between two uprights, measured from the circular arc with above curvature (Fig. 43), we have:

$$\frac{d\eta_O}{dx_O} = \frac{dX_O}{dx_O} + x_O \frac{\epsilon_{x_O} - \epsilon_{x_U}}{h} \qquad (50)$$

Then we define (See Figs. 43 and 43) angle φ, at which the connecting line $\overline{OU}$ of the tension diagonal through M is dis-

torted under stress. This angle is caused - first, by the deflection of the whole girder (Fig. 43); this part ϑ_1 amounts to $x_m \dfrac{d^2 \chi_m}{dx_m^2}$, that is, $\vartheta_1 = -\dfrac{x_m}{h}(\epsilon_{x_O} - \epsilon_{x_U})$; second, the other distortions of point O and U produce a distortion ϑ_2 in this connecting line. Now, it becomes apparent from Figures 45 and 45a* that

$$- \vartheta_2 \frac{h}{\sin \alpha} \sin \alpha = \gamma\, h + \frac{\epsilon_{x_O} + \epsilon_{x_U}}{2}\, h \cot \alpha - \lambda \cos \alpha .$$

Here γ is the angle of displacement due to the cross stress, λ the elongation of the tension diagonal due to their stresses σ, and the total distortion becomes

$$\vartheta = \vartheta_1 + \vartheta_2 = -\frac{x_m}{h}(\epsilon_{x_O} - \epsilon_{x_U}) - \gamma -$$

$$-\frac{\epsilon_{x_O} + \epsilon_{x_U}}{2} \cot \alpha + \frac{\lambda}{h} \cos \alpha \tag{51}$$

Thus $\omega_O = \dfrac{d\chi_O}{dx_O}$ (Fig. 43) becomes the angle of the direction of the upper spar at point O after deformation of the girder and the direction of this spar prior to deformation. Consequently, we have with equation (46c)

$$\frac{d\chi_O}{dx_O} = \vartheta - \left(\frac{\partial \mu}{\partial z}\right)_O + \gamma\, \alpha_O$$

and, with (50)

$$\frac{d\eta_O}{dx_O} = x_O \frac{\epsilon_{x_O} - \epsilon_{x_U}}{h} + \vartheta - \left(\frac{\partial \mu}{\partial z}\right)_O + \gamma\, \alpha_O .$$

---

*Since the following equation for ϑ_2 was derived from Figures 45 and 45a, respectively, by projecting the separate displacements on direction x, the η and χ displacements do not occur, and are therefore not specially indicated.

Noting

$$\frac{x_0 - x_m}{h} = \tfrac{1}{2} \cot \alpha$$

we insert value ϑ from (51) and have:

$$\frac{d\eta_0}{dx_e} = - \epsilon_{x_U} \cot \alpha - \gamma + \lambda \cos \alpha - \left(\frac{\partial \mu}{\partial z}\right)_0 + \gamma \, \alpha_0 \qquad (52)$$

Into this equation (53) we write the value for γ conformal to (40a), the value for $\left(\frac{\partial \mu}{\partial z}\right)_0$ according to (44), for $\gamma \alpha_0$ as given in (46a) $(\alpha_0 = \alpha)$ so that our final equation (Note also (48) and (37a)) reads:

$$\frac{d\eta_0}{dx_0} = - \gamma - 2 \cot \alpha \, \frac{\epsilon_{x_0} + \epsilon_{x_U}}{2} +$$

$$+ \, 2 \, \epsilon_m \cot \alpha \, \frac{1}{2r_1} \ln\left(\frac{1 + r_1}{1 - r_1}\right) +$$

$$+ \, \frac{h}{2 \sin^2 \alpha} \, \frac{d\epsilon}{dx_m} \, \frac{1}{r_1} \left[\frac{1}{1 - r_1} - \frac{1}{2r_1} \ln\left(\frac{1 + r_1}{1 - r_1}\right) \right] \qquad (53)$$

In like manner, we obtain:

$$\frac{d\eta_U}{dx_U} = - \gamma - 2 \cot \alpha \, \frac{\epsilon_{x_0} + \epsilon_{x_U}}{2} +$$

$$+ \, 2 \, \epsilon_m \cot \alpha \, \frac{1}{2r_1} \ln\left(\frac{1 + r_1}{1 - r_1}\right) +$$

$$+ \, \frac{h}{2 \sin^2 \alpha} \, \frac{d\epsilon}{dx_m} \, \frac{1}{r_1} \left[\frac{1}{1 + r_1} - \frac{1}{2r_1} \ln\left(\frac{1 + r_1}{1 - r_1}\right) \right] \qquad (53)$$

whereby

$$r_1 = \frac{h}{2 \sin^2 \alpha} \, \frac{d\alpha}{dx_m} = - \frac{h}{2} \, \frac{d \cot \alpha}{dx_m} \qquad (53a)$$

This gives us the desired connection between ϵ_m and α with re-

spect to x_m and the spar deflections. If, in addition, the elastic lines of the spars are given and it is desired to find the produced diagonal tension field, the two equations above - (53) and (53a) - together with (49), suffice for computing ϵ_m and α with respect to x_m.

Lastly, if the elastic lines of the spars are not given but are to be defined conformal to stresses p_{y_O} and p_{y_U} (Compare Part I - Technical Memorandum No. 604 - page 23, and Figure 9, for example, $p_{y_U} = s \sin^2 \alpha \, \sigma_u = s \sin^2 \alpha \, E \frac{\epsilon_m}{1 + r_1}$) we apply in addition to (53), (53a) and (49) the two differential equations for the elastic lines of the spars

$$\frac{d^4 \eta_O}{dx_O^4} = - \frac{s \sin^2 \alpha \, \epsilon_m}{(1 - r_1) \, J_O} \tag{54a}$$

$$\frac{d^4 \eta_U}{dx_U^4} = + \frac{s \sin^2 \alpha \, \epsilon_m}{(1 + r_1) \, J_U} \tag{54b}$$

(J_O, J_U = inertia moments of the spar cross sections; s = sheet thickness.)

Altogether, we have now 7 equations for x_O, x_U, r_1, ϵ_m, α, η_O and η_U.

For later purposes, we subtract the two equations (53), and have:

$$\frac{d \eta_O}{dx_O} - \frac{d \eta_U}{dx_U} = \frac{h}{\sin^2 \alpha} \frac{d \epsilon}{dx_m} \frac{1}{1 - r_1^2} \tag{53b}$$

I have not yet carried through the numerical evaluations

of equations (53) etc.* We have yet to consider the case where α and ϵ_m are constant. Then $\epsilon = \epsilon_m$ becomes constant in the whole range of the sheet; further, $\frac{d\epsilon}{dx_m} = 0$ and $r_1 = 0$, which, written in (53) and added becomes:

$$\frac{1}{2}\left(\frac{d\eta_0}{dx_0} + \frac{d\eta_U}{dx_U}\right) = -\gamma - 2\cot\alpha \frac{\epsilon_{x_0} + \epsilon_{x_U}}{2} +$$

$$+ 2\epsilon\cot\alpha = \text{constant} \qquad (55a)$$

When subtracted,

$$\frac{1}{2}\left(\frac{d\eta_0}{dx_0} - \frac{d\eta_U}{dx_U}\right) = 0 \qquad (55b)$$

For two linear differential equations of the first order we usually apply two limit equations. But equations (53) for η_0 and η_U already satisfy one limit equation inasmuch as we wrote the value for λ into (52) according to (40a) instead of expressing it generally by ϵ_{x_0}, ϵ_{x_U}, λ, ϵ_v, and η_0, η_u. The other limiting condition is expressed by observing the connection (46c) [or (46d)] and complying with (46a), (46b) at one place. In one case of (55a), (55b) it yields:

$$\frac{d\eta_0}{dx_0} + \frac{d\eta_U}{dx_U} = 0$$

---

*If, by given elastic lines of the spars, these deflections η_0 and η_u are small enough so that the stress fluctuations $\left(\frac{d\sigma}{dx_m}\right)$ and the variations in direction of wrinkling (r_1) become (infinitely) small quantities, then η_0 and η_u as well as σ_m and α with respect to x_m may be expressed by Fourier series, which inserted in the two equations (53) yield the indeterminate coefficients of the series for σ_m and α. The result is the stress distribution. But the mathematical results are too complicated to be cited in this report.

Hence, according to (55a), (55b)

$$\frac{d\eta_O}{dx_O} = 0; \quad \frac{d\eta_U}{dx_U} = 0; \quad \gamma = 2 \cot \alpha \left(\epsilon - \frac{\epsilon_{x_O} + \epsilon_{x_U}}{2} \right) \qquad (55c)$$

This equation (55c) (Compare equation (6), - Part I (Technical Memorandum No. 604, page 22)) proves the accuracy of our statement made at the end of an earlier section (Part I, page 29), namely, that α depends on the mean elongation of both spars only.

In particular, we want to point out that, through (53) and (55), spars which by the deformation remain straight and parallel, are given constant wrinkling direction, which in previous sections we had assumed as obvious (See Part I, pages 16 and 23).

Sheet Metal Girder with Spars not Rigid in Bending; Simplifying Assumptions

Again we assume the angle of displacement γ, the elongation ϵ_{x_O} and ϵ_{x_U} of the two spars and the elongation ϵ_v of the uprights as given.

Case 1:

What are the results if the direction of the wrinkles is constant (α = constant)? Noting (37a) $(\sigma_O = \sigma_U = \sigma_m = \sigma)$ equation (53b) becomes:

$$\frac{d\eta_O}{dx_O} - \frac{d\eta_U}{dx_U} = \frac{h}{E \sin^2 \alpha} \frac{d\sigma}{dx_m},$$

we integrate with (49) as

$$\eta_O - \eta_U = \frac{h}{E \sin^2 \alpha} (\sigma - \sigma_g) = \frac{h}{\sin^2 \alpha} (\epsilon - \epsilon_g) \qquad (56)$$

Here σ_g is the integration constant for $\sigma = \sigma_g$ when $\eta_O - \eta_U = 0$. Now we presume that the tension diagonals (stress trajectories) emanating from the junction points of the lower spar (i.e., points of attachment of the uprights) pass also through the junction points of the upper spar (Fig. 46). Then a subtraction of both equations (54) yields:

$$\frac{d^4 (\eta_U - \eta_O)}{d x^4} = s \sin^2 \alpha \, \epsilon \left(\frac{1}{J_O} + \frac{1}{J_U} \right)$$

Now we insert ϵ of (56), place the source $x = 0$ in a junction point and obtain:

$$\frac{d^4 (\eta_U - \eta_O)}{d x^4} = \left(\frac{1}{J_O} + \frac{1}{J_U} \right) s \sin^2 \alpha \, \epsilon_g -$$

$$- \left(\frac{1}{J_O} + \frac{1}{J_U} \right) \frac{s \sin^4 \alpha}{h} (\eta_U - \eta_O) \qquad (57)$$

This is the well-known differential equation of the elastic line of a flexibly supported railroad sleeper, so we may omit the general data. We put the limiting conditions (as long as $\sigma_g \geqq \frac{\sin^2 \alpha}{h} (\eta_U - \eta_O)_{max}$

$$\eta = 0 \quad \text{for} \quad x = 0$$
$$\frac{d\eta}{dx} = 0 \quad " \quad x = 0$$
$$\eta = 0 \quad " \quad x = t$$
$$\frac{d\eta}{dx} = 0 \quad " \quad x = t$$

We denote with

$$\omega t = t \sin \alpha \sqrt[4]{\left(\frac{1}{J_O} + \frac{1}{J_U} \right) \frac{s}{4 \, h}} \qquad (59)$$

and obtain, for example, for maximum deflection in both spars

$$(\eta_U - \eta_0)_{max} =$$

$$= \frac{\epsilon_g \, h}{\sin^2 \alpha} \left(1 - \frac{\sin \frac{\omega t}{2} \cos \frac{\omega t}{2} + \cos \frac{\omega t}{2} \sin \frac{\omega t}{2}}{\sin \frac{\omega t}{2} \cos \frac{\omega t}{2} + \sin \frac{\omega t}{2} \cos \frac{\omega t}{2}} \right)$$

If the spars were rigid in bending the sheet would be sub-jected to a constant tension stress σ, which, computed from the cross stress Q of the sheet metal girder (equation (9)), amounts to

$$\sigma = \frac{2 \, Q}{h \, s} \frac{1}{\sin 2 \alpha} .$$

On account of the deflection in the spars not rigid in bending, the tension stress is, as shown, uneven, and it becomes readily apparent that the mean tension stress σ_{mean} in the sheet would have to become equal to $\frac{2 \, Q}{h \, s} \frac{1}{\sin 2\alpha}$;   that, in fact

$$\sigma_{mean} = \frac{1}{t} \int_0^t \sigma \, d \, x = \frac{2 \, Q}{h \, s} \frac{1}{\sin 2 \, \alpha}$$

The resolution of (57) yields the stresses σ as functions of x, so this integral can be evaluated; the maximum tension stress σ_g becomes

$$\sigma_g = \frac{2 \, Q}{h \, s} \frac{1}{\sin 2 \, \alpha} \frac{\sigma_g}{\sigma_{mean}}$$

with

$$\frac{\sigma_g}{\sigma_{mean}} = \frac{\omega \, t}{2} \frac{\sin \omega \, t + \sin \omega \, t}{\cos \omega \, t - \cos \omega \, t}$$

Now the maximum bending moments M_H in the spar at the up-right and in the center of the field can be calculated.

It will be readily seen that part of the sheet metal is not

stressed when the spacing of the supports is large with respect to the spar stiffness and the girder height. Individual diagonal ties only are being stressed (Fig. 47a), when

$$\omega t \gtreqqless 4.710;$$

in that case the limiting conditions for the differential equations must be modified. We forego a discussion of these simple, but drawn-out calculations, and merely give the most prominent data.

Assuming that the wrinkles (stress trajectories) emanating from the junction points pass through the junction points of the upper spar also and the direction of the wrinkles as constant

$$\omega t = t \sin \alpha \sqrt[4]{\left(\frac{1}{J_O} + \frac{1}{J_U} \right) \frac{s}{4\,h}}$$

yields:

a)   The mean skin stress —

$$\sigma_{mean} = \frac{2}{h} \frac{Q}{s} \frac{1}{\sin^3 \alpha}$$

b)   The maximum skin stress —

$$\sigma_g = \sigma_{mean} \frac{1}{\left(\frac{\sigma_{mean}}{\sigma_g} \right)},$$

where $\frac{\sigma_{mean}}{\sigma_g}$ is read from Figure 48. Closely approximated, we have

$$\frac{\sigma_{mean}}{\sigma_g} = 1 \quad \text{for} \quad 0 \leqq \omega t \leqq 2,$$

$$\frac{\sigma_{mean}}{\sigma_g} = \frac{2}{\omega t} \quad \text{for} \quad 2 \leqq \omega t \leqq \infty,$$

c)   The maximum bending moment of the spars at the junc-
tion points is

$$M_{H_{max}} = Q \frac{t}{h} \tan \alpha \frac{t}{12} C$$

C to be taken from Figure 48. Closely approximated, we write

$$C = 1 \quad \text{for} \quad 0 \leqq \omega t \leqq 3,$$

$$C = \frac{3}{\omega t} \quad \text{"} \quad 3 \leqq \omega t \leqq \infty;$$

d)   Piece l_1 of the spar at which (by relatively low
stiffness in bending) the tension stresses of
the web plate apply (Figs. 47a, 47b):

$$l_1 = \psi t$$

ψ taken from Figure 48.

Case 2:

The two differential equations of the elastic line of the
spars are generally written as

$$\frac{d^4 \eta_O}{dx_O^4} = - \frac{s \, \sigma_O \, \sin^2 \alpha}{E \, J_O} = - \frac{s \, \epsilon_O \, \sin^2 \alpha}{J_O},$$

$$\frac{d^4 \eta_U}{dx_U^4} = + \frac{s \, \sigma_U \, \sin^2 \alpha}{E \, J_U} = + \frac{s \, \sigma_U \, \sin^2 \alpha}{J_U}.$$

Now we assume the spacing of the uprights to be wide in re-
lation to the girder height (Fig. 49), so that $t \gg h$. Then
quantity $\epsilon \sin^2 \alpha$ may be considered as being equivalent in
upper and lower spar for related values of x_O and x_U. In ap-
proximation we make $x_O = x_U$ and subtract the two equations:

$$\frac{d^4 (\eta_U - \eta_0)}{d x^4} = s \left(\frac{1}{J_0} + \frac{1}{J_U} \right) \epsilon \sin^2 \alpha \qquad (59)$$

The value $\epsilon \sin^2 \alpha$ is no constant; moreover, ϵ and α are affected, according to equations (4a) and (4b) (Part I) for given γ and ϵ_x, by the change in spar distance (that is, by any change in ϵ_y). As a matter of fact, we must insert

$$\epsilon_y = \epsilon_v + \frac{\eta_0 - \eta_U}{h}$$

(ϵ_v = elongation of uprights)

at a point x for ϵ_y conformably to the additional approach of both spars due to their deflection between two uprights, when ϵ_1 and α_1 are the values which (4b) and (4a) yield for γ, ϵ_v, and ϵ_x. Then a differentiation, according to ϵ_y produces from (4a), (4b)

$$\frac{d (\epsilon \sin^2 \alpha)}{d \epsilon_y} = \sin^2 \alpha \left[1 + \frac{\cos^2 \alpha}{\frac{2 \epsilon}{\epsilon_x + \epsilon_y} - 1} \right] \qquad (60)$$

and (59) becomes

$$\frac{d^4 (\eta_U - \eta_0)}{d x^4} = s \left(\frac{1}{J_0} + \frac{1}{J_U} \right) \epsilon_1 \sin^2 \alpha_1 -$$

$$- s \left(\frac{1}{J_0} + \frac{1}{J_U} \right) \frac{d (\epsilon \sin^2 \alpha)}{d \epsilon_y} \frac{1}{h} (\eta_U - \eta_0) \qquad (61)$$

But this, aside from the value of the constants, is precisely the same differential equation as before and yields the same solutions when in place of ωt, we write

$$\omega t = t \sqrt[4]{\frac{d (\epsilon \sin^2 \alpha)}{d \epsilon_y} \left(\frac{1}{J_0} + \frac{1}{J_U} \right) \frac{s}{4 h}} \qquad (62)$$

By observing equations (58) and (60), we have:

$$\frac{(\omega t) \text{ case } 2}{(\omega t) \text{ case } 1} = \sqrt[4]{1 + \frac{\cos^2 \alpha}{\dfrac{\dfrac{2 \epsilon}{\epsilon_x + \epsilon_y} - 1}{\sin^2 \alpha}}}$$

Because $(\epsilon_x + \epsilon_y)$ is always negative, the numerator of the fraction is always less than 1, so practical cases are approximated at

$$\frac{(\omega t) \text{ case } 2}{(\omega t) \text{ case } 1} < \sqrt{\frac{1}{\sin \alpha}} = \sim 1.25 \qquad (62a)$$

α being assumed around 40°. The data in Figure 48 are therefore applicable with the value ωt, according to (60), which does not differ very much from ωt according to (58) to this case of plate wall with widely spaced uprights.

Thus far our discussion has centered around approximate solutions of equation (53) with two specific assumptions (cases 1 and 2). With respect to stressed skin (i.e. $\dfrac{\sigma_{\text{mean}}}{\sigma_g}$), case 2 was less favorable because it yielded a higher ωt, that is, a higher σ_g for the same dimensions of the sheet wall. And, having been unable to find a more unfavorable assumption for σ_g, my advice is to figure this value approximately at

$$\omega t = 1.25 \ t \sin \alpha \sqrt[4]{\frac{s}{(J_O + J_U)h}} \qquad (63)$$

With respect to bending stresses in the spar (i.e., value C), case 1 was less favorable, because this stress decreases as ωt increases. But according to my calculations it appears

as if this stress were still higher than that computed for case 1, when the wrinkle, emanating from the lower spar at the junction with the upright, meets the upper spar between two uprights.

Inasmuch as the exact moment of this stress in bending is not paramount in correctly constructed sheet metal girders, and since its effect is secondary in importance as compared with the allowable resultant stress in bending and compression for the spars, I deem it best to express the bending in the spar simply by the highest possible $M_{H_{max}} = \frac{Vt}{12}$ (that is, $C = 1$).

Example

Let us check the effect of the flexibility in bending of the spars (Fig. 50) on the example of a previous section (Part I, T.M. No. 604, page 29):

$$Q = 8000; \quad h = 60 \text{ cm}; \quad t = 25 \text{ cm}; \quad s = 0.1 \text{ cm};$$
$$\alpha = 39.5^{\circ}; \quad \sin \alpha = 0.646.$$

To emphasize this effect, we determine the cross-sectional area at section I (Fig. 50), because here the spars are still very weak; the first bay alongside the point of application of the cross stress Q, where the spars are still weaker, is out of the question because it would entail special provisions to ensure the lateral bending stiffness of the outside vertical (Fig. 47). According to equation (13c) (Part I), the spar stresses are

$$H_{O,U} = \pm \frac{8000 \text{ x}}{60} - 0.6 \times 8000$$

and $H_O = + 200;$ $H_U = - 9800$

for $x = 37.5,$

   With a $- 2000$ kg/cm³ allowable stress for the lower spar,
we select, for example, two angle sections 45 × 2.8 mm, whose
total inertia moment is $J_U = 10$ cm⁴. For the upper spar, which
is only under 200 kg tension at this point, we choose a cross
section at least equivalent by $x = 0,$ that is, for 4800 kg
compression (by alternating direction of cross stress Q we
would have to define F_O and J_O in conformity with this other
load case for compression stresses). Accordingly, we may assume
$J_O = 7$ cm⁴.

   Now equation (63) yields:

$$\omega t = 1.25 \times 25 \times 0.636 \sqrt[4]{\frac{0.1}{(7 + 10)\, 60}} = 1.98$$

and Figure 48:

$$\frac{\sigma_{mean}}{\sigma_g} = 0.92 \quad C = 0.98.$$

   So, since the maximum tension stress σ_g in the sheet is
8 per cent higher than the mean stress σ_{mean} the yield limit
is already reached at an 8 per cent lower load. But these stress
differences become neutralized upon exceeding the yield limit,
so the ultimate load of the flexible spars is in no wise altered
by this effect (See page 10 of this report, "Exceeding the Yield
Limit").

   If we take care to prevent a premature excess of yield lim-

it, we can, without increasing the weight, reduce the spacing of the upright to perhaps 17 cm. Then, $\omega t = 1.35$ which, according to $\dfrac{\sigma_{mean}}{\sigma_g} = 0.98$ in Figure 48, raises the stress only 2 per cent.

The bending moment in the spar which, with $C = 0.98$ is only 2 per cent lower than $\dfrac{Vt}{12}$, can always be figured at $M_{H_{max}} = \dfrac{Vt}{12}$ $(C = 1)$. In the panels farther to the right (Fig. 50) the spars are stiffer yet, so that any check at these places is superfluous.

The relations set up with the simplified assumptions in this paragraph lead to such simple mathematical data that a certain degree of inaccuracy may well be taken in the bargain.

Translation by J. Vanier,
National Advisory Committee
for Aeronautics.
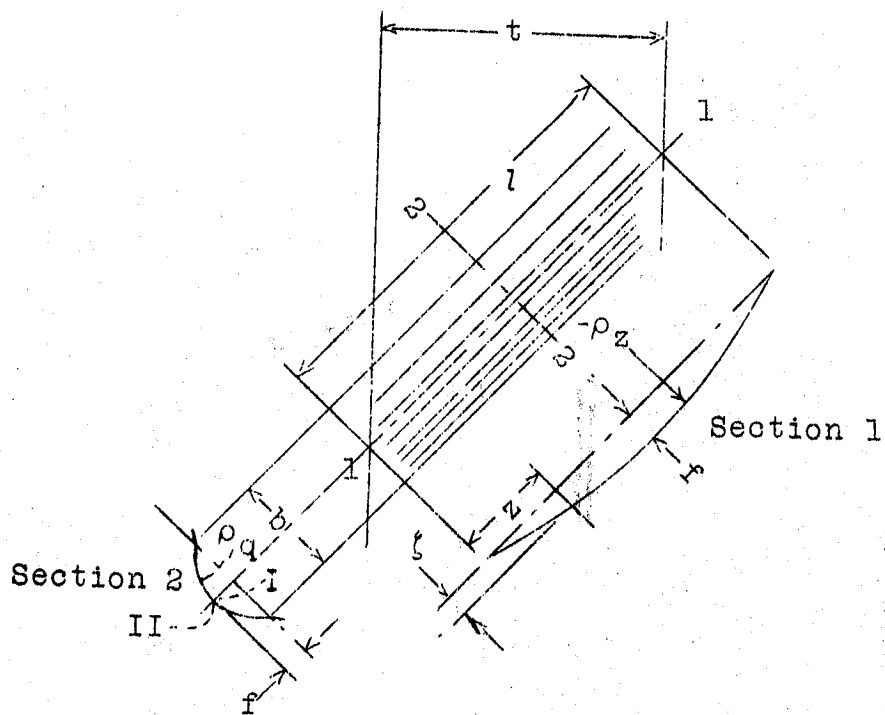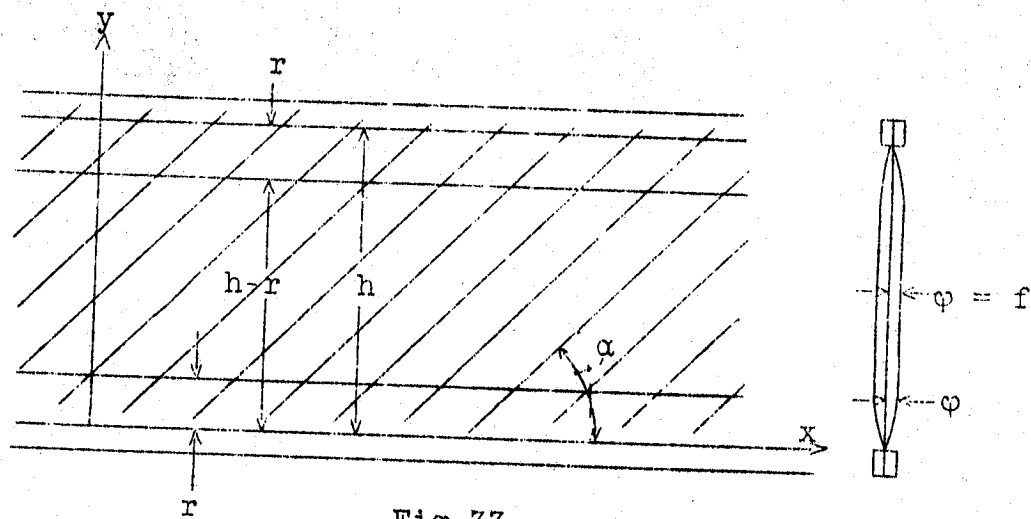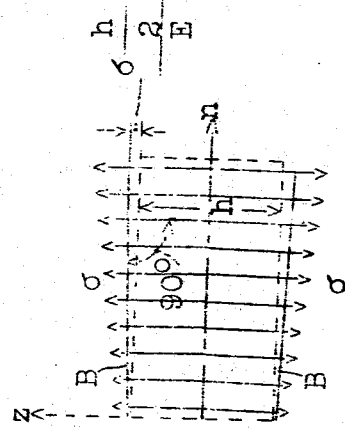
Fig.33
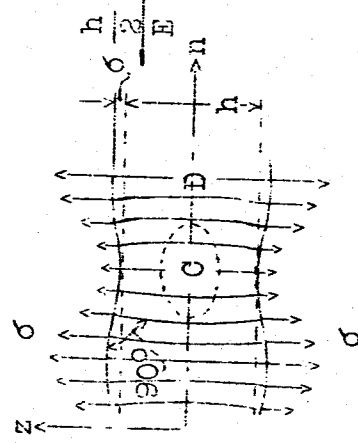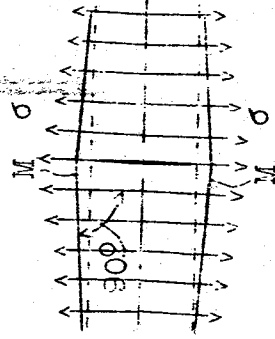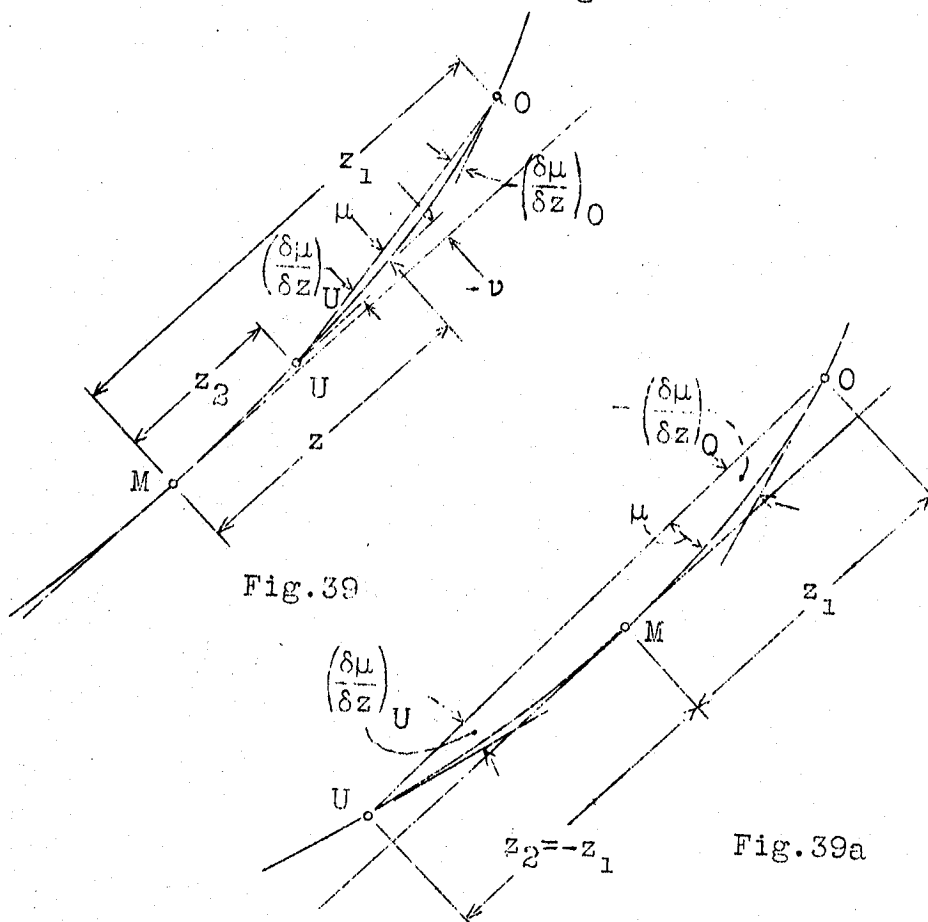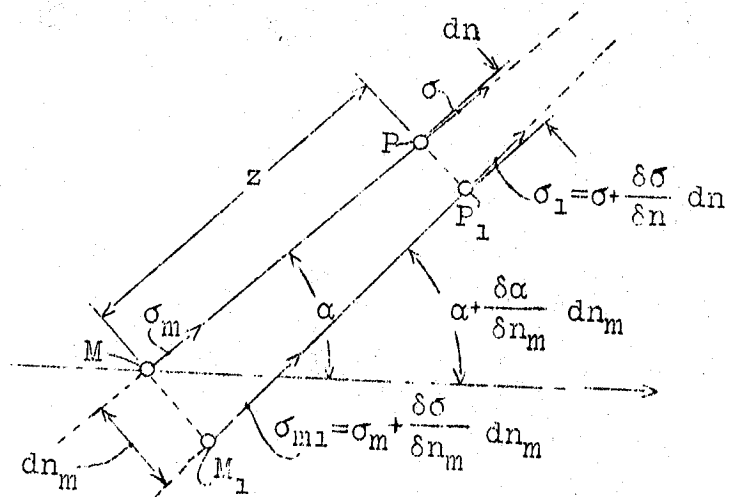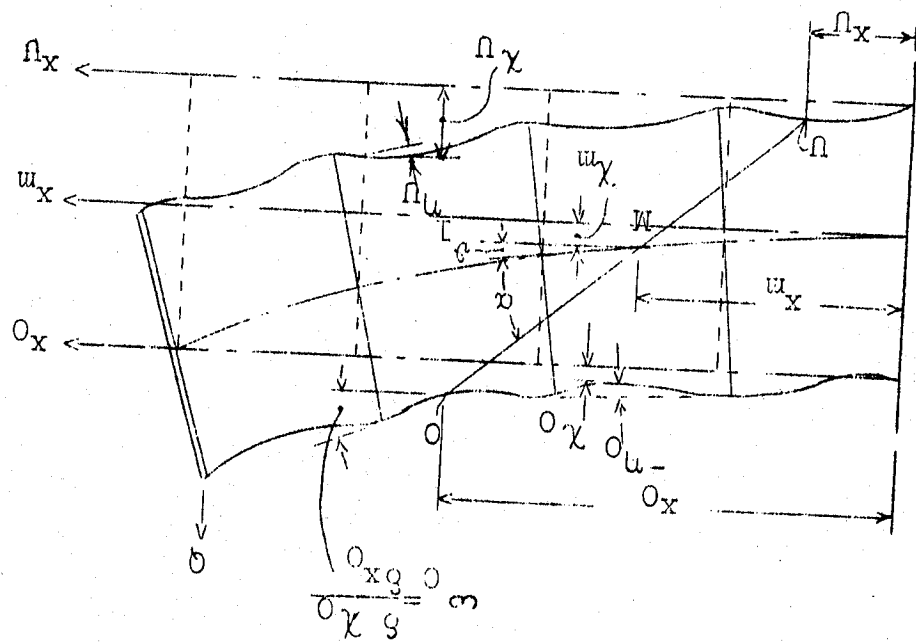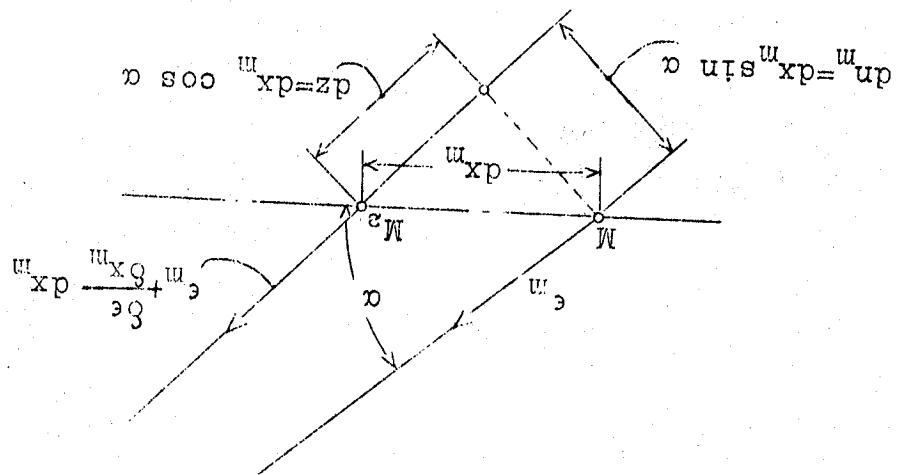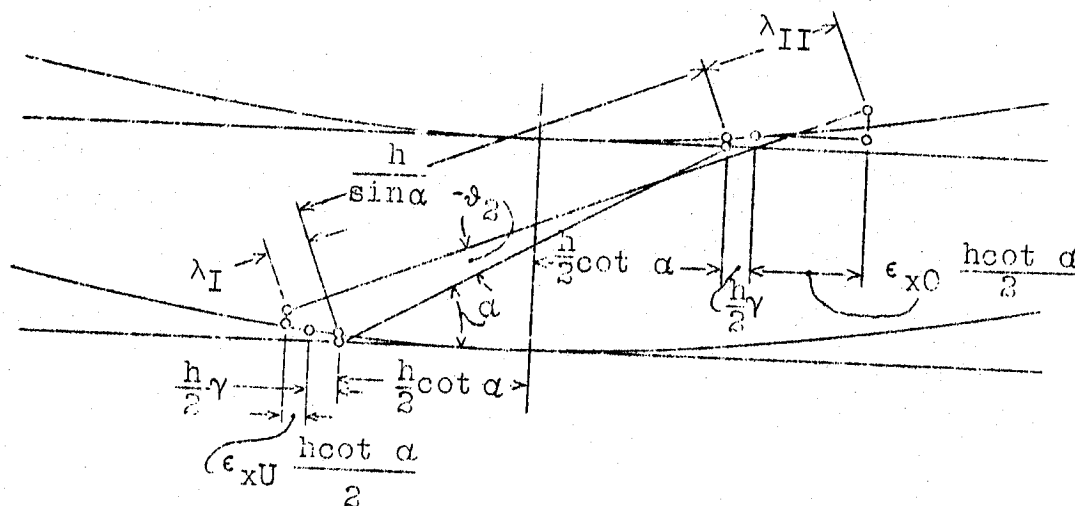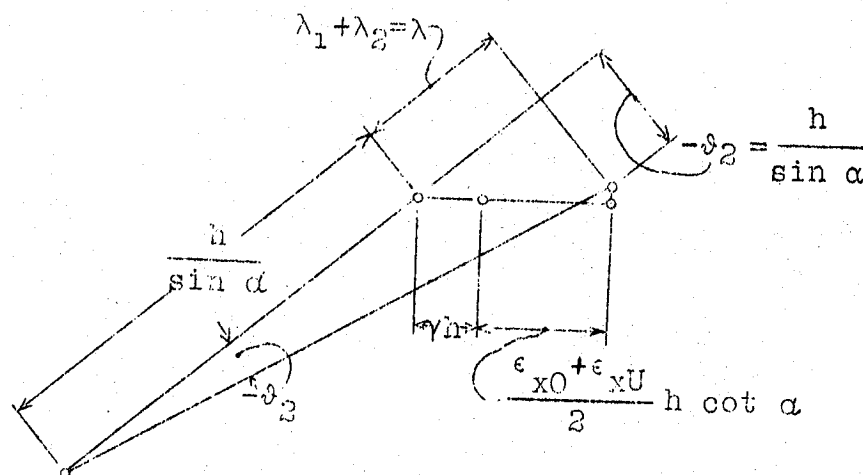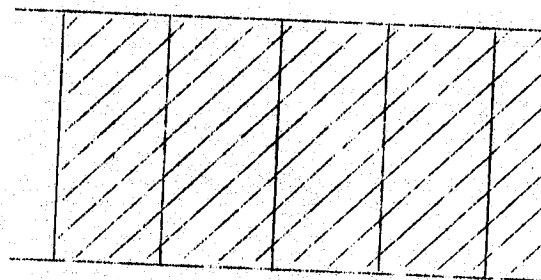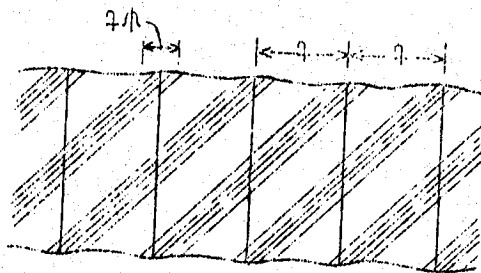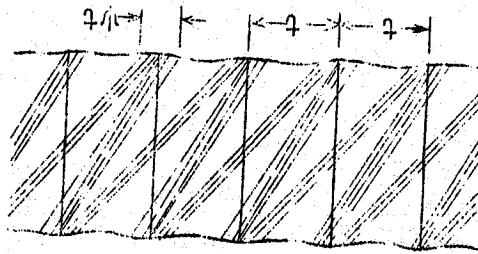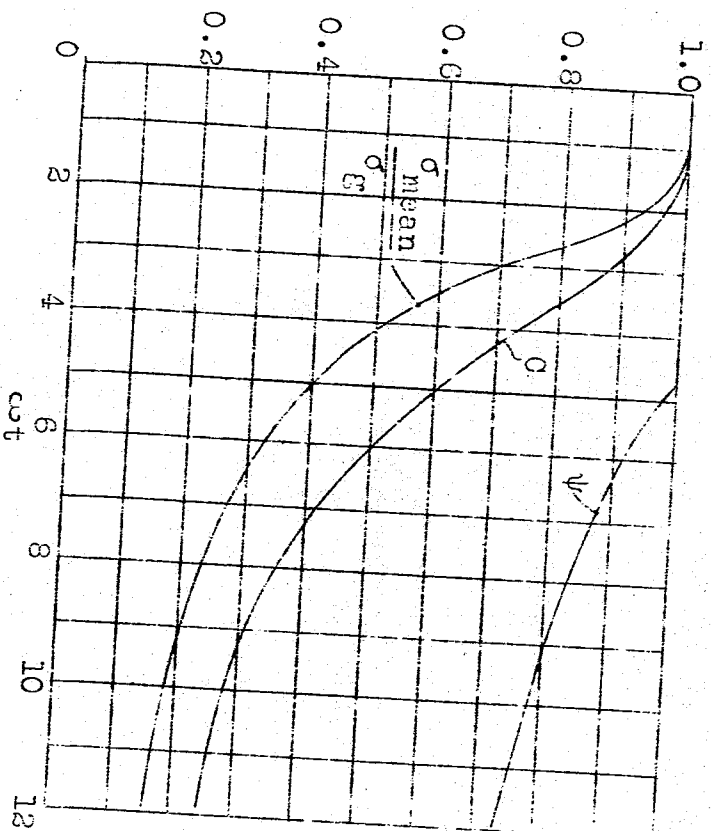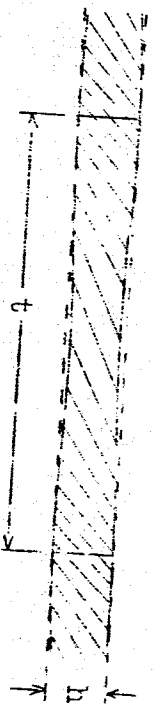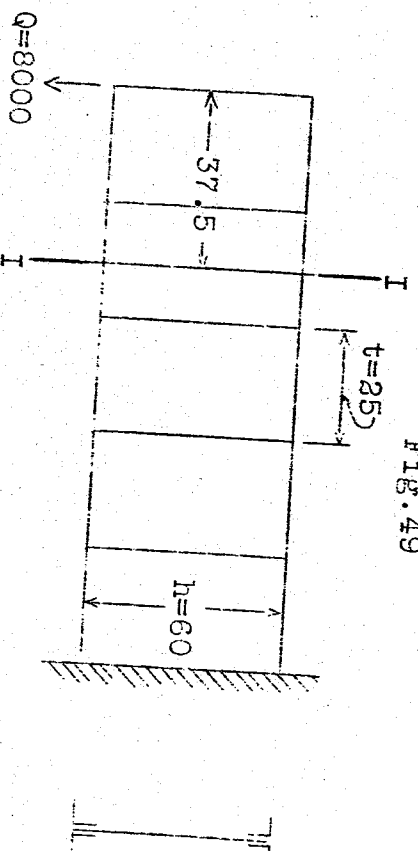
Fig.34

Fig.35

Fig.36

Fig.37

$$\sigma_1 = \sigma + \frac{\delta\sigma}{\delta n} \, dn$$

$$\alpha + \frac{\delta\alpha}{\delta n_m} \, dn_m$$

$$\sigma_{m1} = \sigma_m + \frac{\delta\sigma}{\delta n_m} \, dn_m$$

Fig.38

$$\left(\frac{\delta\mu}{\delta z}\right)_0$$

$$\left(\frac{\delta\mu}{\delta z}\right)_U$$

Fig.39

$$-\left(\frac{\delta\mu}{\delta z}\right)_0$$

$$\left(\frac{\delta\mu}{\delta z}\right)_U$$

$$z_2 = -z_1$$

Fig.39a

Fig. 40

Fig. 41

Fig. 42

Fig.45

Fig.45a

Fig.48

Fig.49

Fig.50

TECHNICAL MEMORANDUMS

NATIONAL ADVISORY COMMITTEE FOR AERONAUTICS

No. 606

FLAT SHEET METAL GIRDERS WITH VERY THIN METAL WEB

By Herbert Wagner

PART III

Sheet Metal Girders with Spars Resistant to Bending
The Stress in Uprights - Diagonal Tension Fields

Washington
February, 1931